Environmental Science & Technology

pubs.acs.org/est

Article

Informing Building Strategies to Reduce Infectious Aerosol Transmission Risk by Integrating DNA Aerosol Tracers with Quantitative Microbial Risk Assessment

Nicholas Clements,* Ilan Arvelo, Phil Arnold, Nicholas J. Heredia, Ulrike W. Hodges, Stan Deresinski, Peter W. Cook, and Kerry A. Hamilton

Cite This: https://doi.org/10.1021/acs.est.2c08131

Read Online

ACCESS | Metrics & More | Article Recommendations | Supporting Information

ABSTRACT: Using aerosol-based tracers to estimate risk of infectious aerosol transmission aids in the design of buildings with adequate protection against aerosol transmissible pathogens, such as SARS-CoV-2 and influenza. We propose a method for scaling a SARS-CoV-2 bulk aerosol quantitative microbial risk assessment (QMRA) model for impulse emissions, coughing or sneezing, with aerosolized synthetic DNA tracer concentration measurements. With point-of-emission ratios describing relationships between tracer and respiratory aerosol emission characteristics (i.e., volume and RNA or DNA concentrations) and accounting for aerosolized pathogen loss of infectivity over time, we scale the inhaled pathogen dose and risk of infection with time-integrated tracer concentrations measured with a filter sampler. This tracer-scaled QMRA model is evaluated through scenario testing, comparing the impact of ventilation, occupancy, masking, and layering interventions on infection risk. We apply the tracer-scaled QMRA model to measurement data from an ambulatory care room to estimate the risk reduction resulting from HEPA air cleaner operation. Using DNA tracer measurements to scale a bulk aerosol QMRA model is a relatively simple method of estimating risk in buildings and can be applied to understand the impact of risk mitigation efforts.

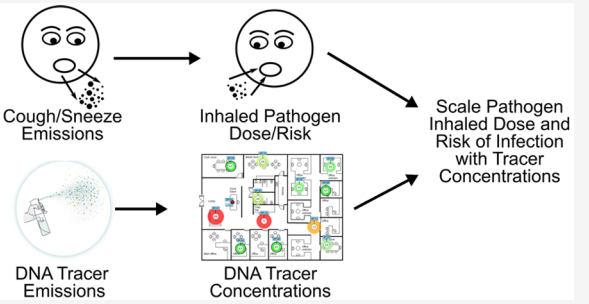

KEYWORDS: *qmra, aerosol tracer, infectious aerosol, aerosol transmission, risk modeling*

1. INTRODUCTION

Inhalation of infectious aerosols can lead to transmission of airborne pathogens,[1] such as SARS-CoV-2[2] and influenza.[3] During the COVID-19 pandemic, organizations such as ASHRAE,[4] AIHA,[5] and WHO[6] released guidance for improving ventilation and filtration systems in buildings and for setting building policies, such as reduced occupancy density and masking, to reduce infectious aerosol exposure. Estimating the extent of risk reduction resulting from implementation of such policies in buildings is a challenge, due partially to the lack of adequate respiratory aerosol exposure proxies. We propose a method for combining airborne pathogen transmission risk modeling and physical tracer measurements for modeling the risk reduction that results from infectious aerosol exposure mitigation measures. This is accomplished by integrating quantitative microbial risk assessment (QMRA)[7−9] with aerosol concentrations of synthetic DNA tracers collected in buildings.[10−12]

QMRA relates an environmental concentration and exposure scenario to a probability of an adverse outcome using a process of hazard identification, exposure assessment, dose−response measurement, and risk characterization.[13] QMRA applied to the inhalation of infectious aerosols estimates transmission risk based on parametrizations of (1) the volume of respiratory aerosol emission, (2) infectious pathogen concentrations and loss of viability and/or infectivity, (3) building operating conditions and policies, (4) inhalation doses, and (5) a dose−response curve, representing a relationship between the dose (i.e., number of pathogens) and the probability of an adverse outcome such as infection, illness, or death.[13] Schijven et al. developed a QMRA model to estimate SARS-CoV-2 aerosol transmission risk,[7] described here as a "bulk aerosol" QMRA model, as once aerosolized pathogen numbers are estimated the particle size distribution is not further considered. Henriques et al. developed a particle size-resolved QMRA model for SARS-CoV-2, increasing the accuracy of the inhalation dose by modeling particle size-dependent emission, transport, and removal.[8,14] Due to the complexity and computational intensity of the particle size-

Received: November 15, 2022
Revised: February 15, 2023
Accepted: March 21, 2023

resolved approach, and due to the use of bulk aerosol collection methods with aerosol tracers, the bulk aerosol QMRA model approach is adopted here. We iterate on the model of Schijven et al., incorporating parametrizations for the survival of pathogens during aerosolization, biological decay of aerosolized pathogens, multiple-occupant scenarios, and interventions such as adding ventilation and masking.

Surrogates for exposure to respiratory aerosols include tracer gases[15−19] and solid particles,[20,21] though tracer gases do not simulate particle evaporation, transport, and removal. Solid particle tracers and particle mass concentration monitoring can indicate how aerosols are dispersed and removed, though these techniques do not simulate the changes in composition and size distribution that respiratory aerosols undergo following emission and evaporation.[22−25] Using an aerosol tracer solution with a composition comparable to that of mucosalivary fluid,[26] it is possible to emulate the physicochemical changes that occur during respiratory aerosol emission and transport. Upon incorporation of a tracer molecule into the liquid aerosol, such as nucleic acid sequences (i.e., synthetic DNA), such a tracer solution becomes quantifiable through quantitative polymerase chain reaction (qPCR). Aerosol tracers tagged with synthetic DNA were originally validated by Harding et al.[10] As currently deployed, a synthetic DNA tracer solution is aerosolized as a burst from a nebulizer, simulating the emission of aerosols similar in composition to and within the size distribution of respiratory aerosols produced during a cough or sneeze.[11]

Presented is a framework for integrating QMRA model estimates of infectious aerosol transmission risk with filter sample-based measurements of aerosolized DNA tracers in buildings to inform the effectiveness of mitigation efforts. We derive a scaling factor for converting from time-integrated aerosolized DNA tracer concentrations to pathogen dose and infection risk using a bulk aerosol QMRA model for SARS-CoV-2. This model is applied for a range of DNA tracer concentrations and modes of emission to analyze the impact of interventions on risk. We apply the framework using modeling parameters from a restaurant outbreak and a case study in an ambulatory care room using real-world measurement data. It is proposed that using aerosol tracer measurements to constrain infectious aerosol risk models is a means of estimating risk-based engineering design parameters in buildings.

2. MATERIALS AND METHODS

2.1. Bulk Aerosol QMRA Model. Equation 1 models the concentration of aerosolized pathogens from a cough or sneeze in a perfectly mixed room

$$n_{pth}(t) = \theta_{inf}(1 - \eta_{msk,out})N_{imp}c_{rsp}\nu_{rsp}\frac{e^{-\lambda_{pth}t}}{\nu_r} \quad (1)$$

where $n_{pth}(t)$ is the concentration of aerosol-bound pathogens (pathogen count per liter of air) in a room with volume ν_r (liters of air), c_{rsp} is the viral load (pathogen count per milliliter of saliva), θ_{inf} estimates the percent of pathogens remaining infectious following aerosolization, $\eta_{msk,out}$ is the bulk aerosol removal efficiency due to the emitter wearing a mask (percent), λ_{pth} is the bulk aerosolized pathogen removal rate (min^{-1}), ν_{rsp} is the volume of respiratory aerosols (milliliters of saliva), and N_{imp} is the number of impulse events. The number of impulse events can be assumed to be from an initial release (i.e., infectious person coughs N_{imp} times) or spaced throughout the exposure time, assuming impulse events are separated by sufficient time for pathogen concentrations to decay to near-background levels between events. We assume a single infectious individual coughs or sneezes at the start of the exposure scenarios, and all other room occupants are non-infectious, breathe at a steady rate, and remain in the room for the duration of the exposure scenario. This model does not estimate the contribution to risk from breathing emissions. The cumulative aerosolized pathogen concentration, N_{pth} (pathogen count-minute per liter of air), is calculated by integrating n_{pth} over an exposure time period [T, minutes (eq 2)].

$$N_{pth}(T) = \int_0^T n_{pth}(t)\,dt = \theta_{inf}(1 - \eta_{msk,out})N_{imp}c_{rsp}\nu_{rsp}\left(\frac{1 - e^{-\lambda_{pth}T}}{\nu_r\lambda_{pth}}\right) \quad (2)$$

The inhaled pathogen dose (D_{pth}, pathogen count) is calculated by multiplying the cumulative aerosolized pathogen concentration by the inhalation rate of a room occupant (q_{inh}, liters of air per minute). Equation 3 includes η_{inh}, the bulk respiratory aerosol lung deposition efficiency (percent), and $\eta_{msk,in}$, the bulk inward mask filtration efficiency (percent).

$$D_{pth}(T) = [\eta_{inh}(1 - \eta_{msk,in})q_{inh}]\left[\theta_{inf}(1 - \eta_{msk,out})N_{imp}c_{rsp}\nu_{rsp}\left(\frac{1 - e^{-\lambda_{pth}T}}{\nu_r\lambda_{pth}}\right)\right] \quad (3)$$

The risk of infection (P_{pth}, percent) of an exposed individual is calculated from a dose−response curve (eq 4).

$$P_{pth}(T) = 1 - e^{-frD_{pth}(T)} \quad (4)$$

Using an RNA-based viral load for pathogen emissions, the f factor converts the inhaled dose from RNA copies to infectious units. The r factor estimates the dose of infectious units leading to infection in half of the population on average. Dose−response parametrization values are based on the work of Schijven et al., with an f factor of 1/80 (PFU/RNA copies) and an r factor of 1/18 (infection/PFU inhaled).[7]

A human challenge study of SARS-CoV-2 infection by Killingley et al. with intranasal droplet inoculation of D614G-containing pre-alpha wild-type virus to healthy SARS-CoV-2 seronegative volunteers without prior vaccination or history of COVID-19 determined the median infectious dose to be 10 $TCID_{50}$, equivalent to 55 FFU (r = 1/55).[27] As Killingley et al. also report the viral load in FFU per milliliter of saliva, we use this viral load parametrization with the FFU-based r factor (f = 1; r = 1/55) to compare to the risk indicated by models using RNA-based viral load values.

We assume the exposed population is fully and equally susceptible to illness, and there are no modifications to the dose−response relationship to accommodate the effects of vaccination or prior infection. Therefore, risk estimates can be considered an upper bound on infection risk for a highly susceptible population. As room occupancy increases, and we assume equal risk to all individuals corresponding to the median exposure dose, the risk that one or more occupants will become infected ($P_{pth,multi}$) follows eq 5

https://doi.org/10.1021/acs.est.2c08131
Environ. Sci. Technol. XXXX, XXX, XXX−XXX

$$P_{\text{pth,multi}} = 1 - (1 - P_{\text{pth}})^{p} \quad (5)$$

where p is the number of exposed occupants.

Section S1 of the Supporting Information describes the modeled respiratory aerosol volume emission distributions, based on distributions reported by Schijven et al.[7] Section S2 describes the viral load distributions.[7,27] Section S3 describes the inhalation rate distribution.[28]

The bulk aerosolized pathogen removal rate (λ_{pth}, eq 6) is the sum of physical and biological removal rates of pathogen-laden aerosols.[8]

$$\lambda_{\text{pth}} = \lambda_{\text{vnt}} + \lambda_{\text{flt}} + \lambda_{\text{dep}} + \lambda_{\text{inh}} + \lambda_{\text{bio}} \quad (6)$$

Physical removal processes include ventilation (λ_{vnt}), filtration (λ_{flt}), deposition (λ_{dep}), and inhalation (λ_{inh}). The biological decay of aerosolized SARS-CoV-2 due to environmental conditions (λ_{bio}) has been assessed in rotating drum aerosol chambers, resulting in a parametrization of the decay constant based on temperature, humidity, and UVB irradiance.[29] We assume an indoor temperature of 23 °C, a relative humidity of 50%, and no sunlight (0 W_{UVB}/m^2), resulting in a decay constant for viral infectivity ($k_{\text{infectivity}}$) of 0.023 min^{-1} (1.4 h^{-1}). Converting from $\log_e$ units results in a biological decay rate [$\lambda_{\text{bio}} = \ln(2)/k_{\text{infectivity}}$] of 0.008 min^{-1} (0.5 h^{-1}), which is comparable to biological decay rates in other risk modeling studies.[8,30] In buildings where the distributions of temperature and humidity are known, these two variables can be sampled during Monte Carlo simulation to quantify the variability in the biological decay rate. Other factors that impact decay of infectivity, such as pH, are not currently incorporated into this model of biological decay.[31,32]

To estimate the inhalation removal rate (eq 7), the inhalation volumetric flow rate was summed across the room occupants (p) and multiplied by factors describing the bulk deposition efficiency of aerosols in the respiratory system (η_{inh}, percent) and the inward mask aerosol filtration efficiency ($\eta_{\text{msk,in}}$, percent) and then scaled by the room volume (v_r, liters of air).

$$\lambda_{\text{inh}} = \frac{\eta_{\text{inh}}(1 - \eta_{\text{msk,in}}) \sum_{1}^{p} q_{\text{inh},i}}{v_r} \quad (7)$$

2.2. Synthetic DNA Tracer Emission and Sampling. The synthetic DNA tracer solution is a nonhazardous aqueous solution (98% water by mass; the composition balance is a trade secret) containing a concentration of synthetic DNA tracers (c_{trc}, DNA copies per milliliter of solution) quantified via qPCR. The tracer solution composition simulates human mucosalivary secretions, composed of ∼99% water and a mixture of salts, proteins, surfactants, and other organic matter.[26] Synthetic DNA tracers do not decay in the environment over time scales used for testing, for example, due to changes in aerosol pH, and are stable during aerosolization. Therefore, tracer concentrations are an upper bound of pathogen transport where biological decay processes do not occur.

The DNA tracer solution is emitted using a pneumatic nebulizer with a known volumetric emission rate.[11] Volumetric particle size distributions upon emission were measured in triplicate 0.15 m from the nebulizer with a Spraytec laser diffraction particle counter (0.12−1000 μm, Malvern Panalytical Ltd.) and converted to normalized particle number concentrations. The average relative particle number distribution of the nebulizer is compared to a normalized distribution from the BLO trimodal model of cough aerosols in Figure S1.[33] Additional analysis of the nebulizer emission characteristics is included in Section S4.

The volume of the tracer solution emitted during each application is typically a few milliliters. We assume the nebulizer emission size distribution measured by the Spraytec is representative of this entire volume (i.e., no droplets of >1000 μm). Not all emitted mass from the nebulizer is aerosolized due to ballistic droplets being removed through gravitational deposition. We define an aerosolization cutoff diameter of 73.5 μm, the estimated cutoff size at which respiratory particles stay aerosolized with assumed conditions of a room temperature of 23 °C, an exhalation velocity of 4.1 m/s, a relative humidity of 50%, and an ambient air velocity of 0.3 m/s.[34] The nebulizer emits 88.5% of the tracer solution volume below the aerosolization cutoff diameter, and the volumetric emission per application (v_{tot}, milliliters of solution per application) is multiplied by this aerosolization fraction (η_{aero}) to estimate the volume of the aerosolized tracer solution emitted per application (v_{trc}, milliliter of solution per application). The number of aerosolized DNA copies emitted per application (e_{trc}, DNA copies per application) is calculated using eq 8. Details of DNA tracer filter sampling and quantification are included in Section S5.[35,36]

$$e_{\text{trc}} = c_{\text{trc}} v_{\text{trc}} = c_{\text{trc}} v_{\text{tot}} \eta_{\text{aero}} \quad (8)$$

2.3. Aerosolized DNA Tracer Removal Rate. Measuring bulk aerosolized DNA tracer removal rates ($\lambda_{\text{trc,meas}}$) in buildings, which accounts for the combined removal rates of ventilation, filtration, and deposition, can be accomplished using aerosolized tracer concentration decay techniques,[11] and we assume bulk aerosolized tracer removal rates are equivalent to bulk respiratory aerosol removal rates due to similarities in particle size distributions and composition. When aerosol tracer decay rates cannot be measured, gaseous tracer removal rates (λ_{gas}) or ventilation rates (q_v/v_r) can be used to estimate tracer aerosol removal rates using the linear regression described in Section S6. The measured or estimated aerosolized DNA tracer concentration removal rate is assumed to be representative of the physical removal from ventilation, filtration, and deposition (eq 9). As aerosolized DNA tracer concentrations are assumed to decay at the same rate as aerosolized pathogen concentrations, λ_{pth} can be estimated by substituting the tracer removal rate for ventilation, filtration, and deposition removal (eq 10).

$$\lambda_{\text{trc}} = (\lambda_{\text{vnt}} + \lambda_{\text{flt}} + \lambda_{\text{dep}}) = \lambda_{\text{trc,meas}} \approx \hat{\lambda}_{\text{trc,chm}}\left(\lambda_{\text{gas}}, \frac{q_v}{v_r}\right) \quad (9)$$

$$\lambda_{\text{pth}} = \lambda_{\text{vnt}} + \lambda_{\text{flt}} + \lambda_{\text{dep}} + \lambda_{\text{inh}} + \lambda_{\text{bio}} = \lambda_{\text{trc}} + \lambda_{\text{inh}} + \lambda_{\text{bio}} \quad (10)$$

2.4. Relating Airborne DNA Tracer Concentration to Infection Risk. Table S4 summarizes point-of-emission ratios for respiratory and tracer aerosols in terms of volume, pathogen/tracer concentration in saliva/solution, and the number of pathogens/tracers emitted, using distribution means of respiratory aerosol emission volume and viral load and typical tracer solution characteristics. To account for the differences in time-integrated pathogen and tracer concentrations, the modeled cumulative pathogen concentration [$N_{\text{pth}}(T)$] is divided by the modeled cumulative tracer

https://doi.org/10.1021/acs.est.2c08131
Environ. Sci. Technol. XXXX, XXX, XXX−XXX

concentration [$N_{trc}(T)$], resulting in the cumulative pathogen tracer concentration ratio [$R(T)$ (eq 11)], which includes the point-of-emission ratios.

$$R(T) = \frac{N_{pth,mod}(T)}{N_{trc,mod}(T)} = \theta_{inf}(1 - \eta_{msk,out}) N_{imp}\left(\frac{c_{rsp}}{c_{trc}}\right)\left(\frac{v_{rsp}}{v_{tot}\eta_{aero}}\right)\left(\frac{\lambda_{trc}}{\lambda_{pth}}\right)\left(\frac{1 - e^{-\lambda_{pth}T}}{1 - e^{-\lambda_{trc}T}}\right) \quad (11)$$

Assuming respiratory and tracer aerosols are transported in a proportionally consistent manner due to similarities in particle size distributions and composition, concentrations of DNA tracers measured on a filter can be proportionally related to the number of pathogens inhaled from a cough or sneeze. To scale the inhaled dose based on measurements of tracer concentrations, the measured cumulative aerosolized tracer concentration ($N_{trc,meas}$), from time-integrated tracer concentrations measured with a filter sampler ($c_{trc,meas}$), can be calculated with the filter sampling time (T, minutes), which is the same as the modeled exposure time (eq 12). To model how interventions that impact the removal rate (λ_{int}) alter pathogen concentrations, we assume that the ratio of measured and modeled cumulative tracer concentrations is consistent as the removal rate changes (eq 13).

$$N_{trc,meas}(\lambda_{trc}, T) = c_{trc,meas}T \quad (12)$$

$$N_{trc,meas}(\lambda_{trc} + \lambda_{int}, T) = N_{trc,mod}(\lambda_{trc} + \lambda_{int}, T)\frac{N_{trc,meas}(\lambda_{trc}, T)}{N_{trc,mod}(\lambda_{trc}, T)} \quad (13)$$

We multiply the pathogen dose equation, with λ_{int} added to the pathogen removal rate, by the tracer scaling factor ($N_{trc,meas}/N_{trc,mod}$), resulting in the tracer-scaled dose equation [D_{trc} (eq 14)].

$$D_{trc}(T) = [\eta_{inh}(1 - \eta_{msk,in})q_{inh,i}]N_{pth,mod}(\lambda_{pth} + \lambda_{int}, T)\left[\frac{N_{trc,meas}(\lambda_{trc} + \lambda_{int}, T)}{N_{trc,mod}(\lambda_{trc} + \lambda_{int}, T)}\right] \quad (14)$$

The tracer scaling factor is the ratio of the measured to modeled cumulative tracer concentrations and represents the proportional deviation from the modeled tracer emission scenario that occurred during transport from emission to sampling point, implicitly including the impact of effects such as mixing effectiveness on the resulting concentrations. $R(T)$ emerges when adopting this convention. Substituting eq 13 for $N_{trc,meas}(\lambda_{trc} + \lambda_{int})$ and eq 12 for $N_{trc,meas}(\lambda_{trc})$ in eq 14 leads to the tracer-scaled dose model parametrized by tracer measurements (eq 15). The tracer-scaled dose is used to calculate the tracer-scaled risk (P_{trc}) using eq 4, and the tracer-scaled risk is used to estimate risk in scenarios with multiple occupants ($P_{trc,multi}$) using eq 5.

$$D_{trc}(T) = [\eta_{inh}(1 - \eta_{msk,in})q_{inh,i}]\left[\frac{N_{pth,mod}(\lambda_{pth} + \lambda_{int}, T)}{N_{trc,mod}(\lambda_{trc}, T)}\right] c_{trc,meas}T \quad (15)$$

2.5. Model Evaluation and Sensitivity Analysis. For each exposure scenario, Monte Carlo simulation (n_{sim} = 10 000) in R[37] was used to evaluate three models during the exposure/filter sampling period (t = 0−T min) using the distributions in Table S5: model 1, the pathogen emission and risk model (n_{pth}, N_{pth}, D_{pth}, and P_{pth}); model 2, the tracer emission model (n_{trc} and N_{trc}); and model 3, the tracer-scaled pathogen dose and risk model (D_{trc} and P_{trc}). Output distributions were statistically summarized with percentiles. We compare the absolute risk across model scenarios, as well as the relative risk (RR) normalized by a baseline model (eq 16).

$$RR = \frac{P_{trc}(\text{comparison model})}{P_{trc}(\text{baseline model})} \quad (16)$$

In scenario testing, we simulate an office-sized space (46.24 m^2 with 2.4 m ceilings) with a typical range of measured tracer concentrations (3.7×10^3, 3.7×10^4, and 3.7×10^5 DNA copies per liter of air) and adjust model inputs over realistic ranges. Each tracer concentration and mode of emission was treated as an independent exposure scenario. The range of tracer concentrations was set such that the tracer scaling factor ranged from 0.0097 to 0.97. The highest tracer concentration value roughly matches the risk of the unscaled pathogen model. It is possible for the tracer scaling factor to be higher than unity, for example, if there is highly directional flow from the emission to sampling points and poor room mixing, leading to less spatial dispersion than assumed in the model with immediate and perfect mixing. We assume a 60 min exposure time with eight impulse events.

The occupant density was assumed to range from low, with one other occupant (23.1 m^2/occupant), to dense, with 30 other occupants (1.5 m^2/occupant). The tracer gas-indicated outdoor air change rate is assumed to be 0.0083 min^{-1} (0.5 h^{-1}), resulting in a tracer removal rate of 0.046 min^{-1} (2.79 h^{-1}). Intervention removal rates ranged from −0.015 min^{-1} (−0.925 h^{-1}), representing only deposition removal with no ventilation, to a high ventilation rate of 0.167 min^{-1} (10 h^{-1}).

Respiratory emission volumes were sampled from a normal distribution of log 10-transformed data (Section S1).[7,38−40] Upon simulation of a multiple-release event (N_{imp} > 1), a single emission volume was sampled and multiplied by the number of impulse events, representing a person who consistently emits the same volume. The viral load was sampled from a normal distribution of log 10-transformed data (Section S2).[7,41] Distributions of viral load and respiratory aerosol volume span multiple orders of magnitude, resulting in a broad range of simulated emitted pathogen numbers. For example, the 10th percentile, median, and 90th percentile of pathogens emitted for the Cough-Hi emission mode for eight emission events were 3.6, 8.9×10^2, and 9.86×10^4 RNA copies, respectively.

Inhalation rates were sampled from a normal distribution for each occupant (Section S3).[28] Ratios of viable virus counts to virus genome equivalents[42] were fit with a beta distribution using the fitdistrplus package in R to estimate the distribution of the percent of pathogens remaining infectious following aerosolization (θ_{inf}). Normal distributions of inward and outward filtration effectiveness for 1.75 μm particles from Koh et al. for a fitted N95 respirator, a surgical mask, and a cloth mask (cloth mask 2, no filter) were used to compare against the data of an unmasked population.[43] The inhalation deposition fraction was based on the sum of the percent deposition into the head airways, tracheobronchial region, and

https://doi.org/10.1021/acs.est.2c08131
Environ. Sci. Technol. XXXX, XXX, XXX−XXX

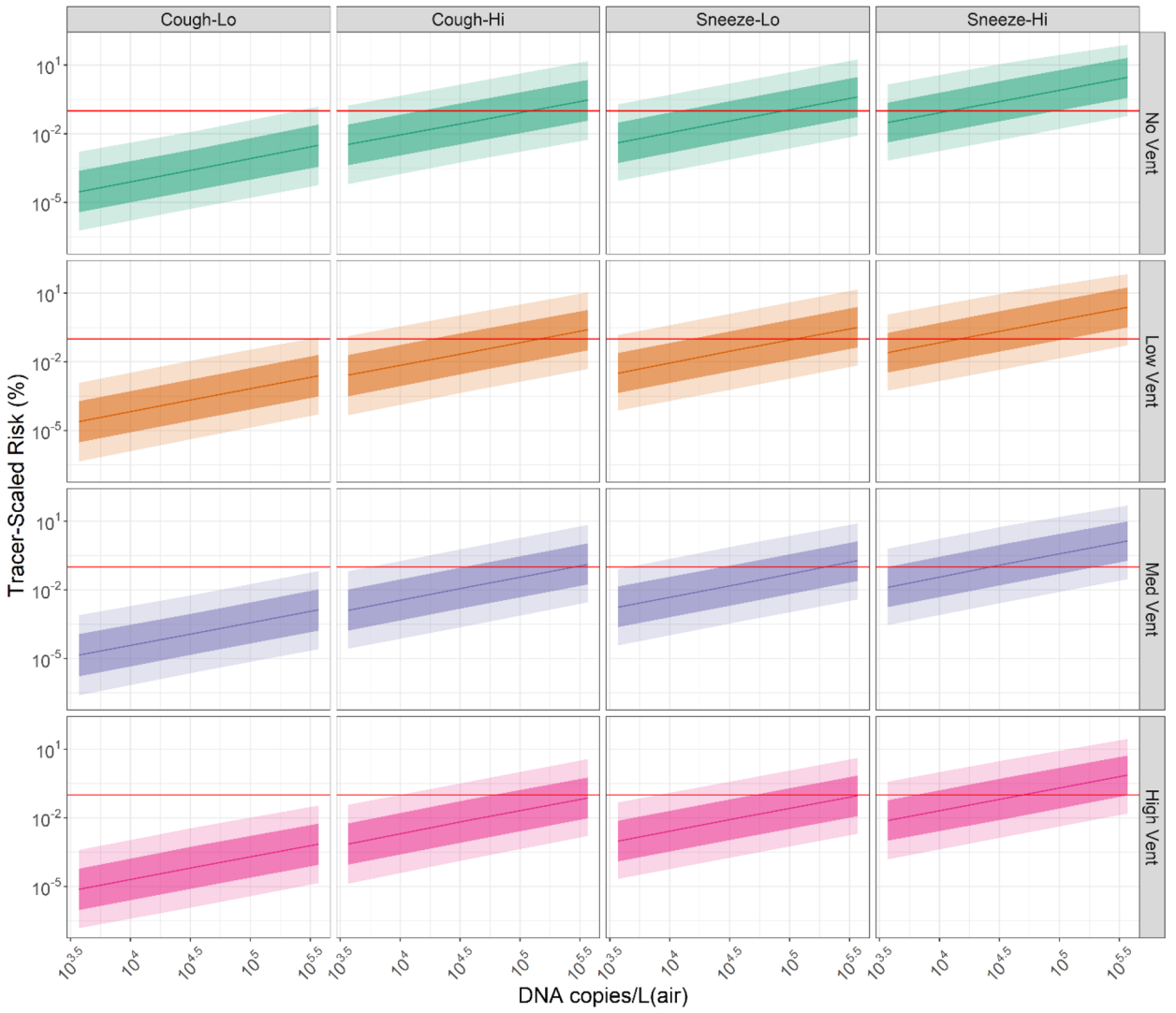

Figure 1. Tracer-scaled risk vs measured tracer concentration as the ventilation rate is varied. The line is the median; the dark ribbon shows the 25th to 75th percentiles, and the light ribbon shows the 10th to 90th percentiles. The horizontal red line indicates 0.1% risk.

alveolar region from Marr et al. for a respiratory aerosol particle initially 10 μm in diameter emitted into a room below 64% relative humidity.[44]

Input−output relationships were assessed with Spearman rank correlations between risk and viral load, emission volume, and the fraction of pathogens surviving aerosolization. Five exposure scenarios were analyzed in which baseline scenario model inputs were held constant (Table S5) while other input variables were manipulated. Scenario testing parameters are included in Table S6. Scenarios were designed to compare the impact of the following factors on risk: (a) ventilation, (b) occupancy, (c) masking, (d) layering interventions, and (e) dose−response curve. For dose−response comparisons, the first two models use an RNA-based viral load and then convert to infectious units with different f factors, and the last two models use an infectious unit-based viral load (FFU per milliliter of saliva) with the f factor set to unity and the same r factors. In dose−response scenario testing, the impact of a high-ventilation intervention was assessed.

Parameters from Parhizkar et al. for a SARS-CoV-2 outbreak that occurred in a restaurant in Guangzhou, China, were used to compare to the predicted risk from the tracer-scaled QMRA model.[45] In this outbreak, 10 of 21 individuals sitting near each other were infected from a single emitter while dining at a restaurant. The high attack rate (47.6%) from this outbreak is attributed to a low outdoor air ventilation rate and exposed individuals sitting in a "bubble" of higher pathogen concentrations created by a recirculating air conditioning unit.[46] We assumed 17.08 L/s of outdoor air supply, a 110 m^3 room volume estimating the bubble dimensions, 20 adult occupants besides the emitter, eight emission events, a 75 min exposure time, an indoor temperature of 23 °C, an indoor relative humidity of 50%, indoor UVB of 0 W/m^2, and the same tracer solution and emission characteristics used in the scenario modeling presented above. The occupant density in this restaurant was 1.55 m^2/occupant, similar to the high-occupant density scenario presented above. We assume measured tracer concentrations of 10^4, 10^5, and 10^6 DNA copies/L of air, corresponding to tracer scaling factors of 0.033, 0.33, and 3.3, respectively. This range of tracer scaling factors was tested due to air flow in this restaurant being highly directional and recirculated via mini-split air conditioning units with little filtration. Poor air mixing between recirculation zones was measured in this restaurant with tracer gas testing; therefore, we estimated that it is conceivable that tracer scaling factors could be greater than unity.[46] The impact of adding

https://doi.org/10.1021/acs.est.2c08131
Environ. Sci. Technol. XXXX, XXX, XXX−XXX

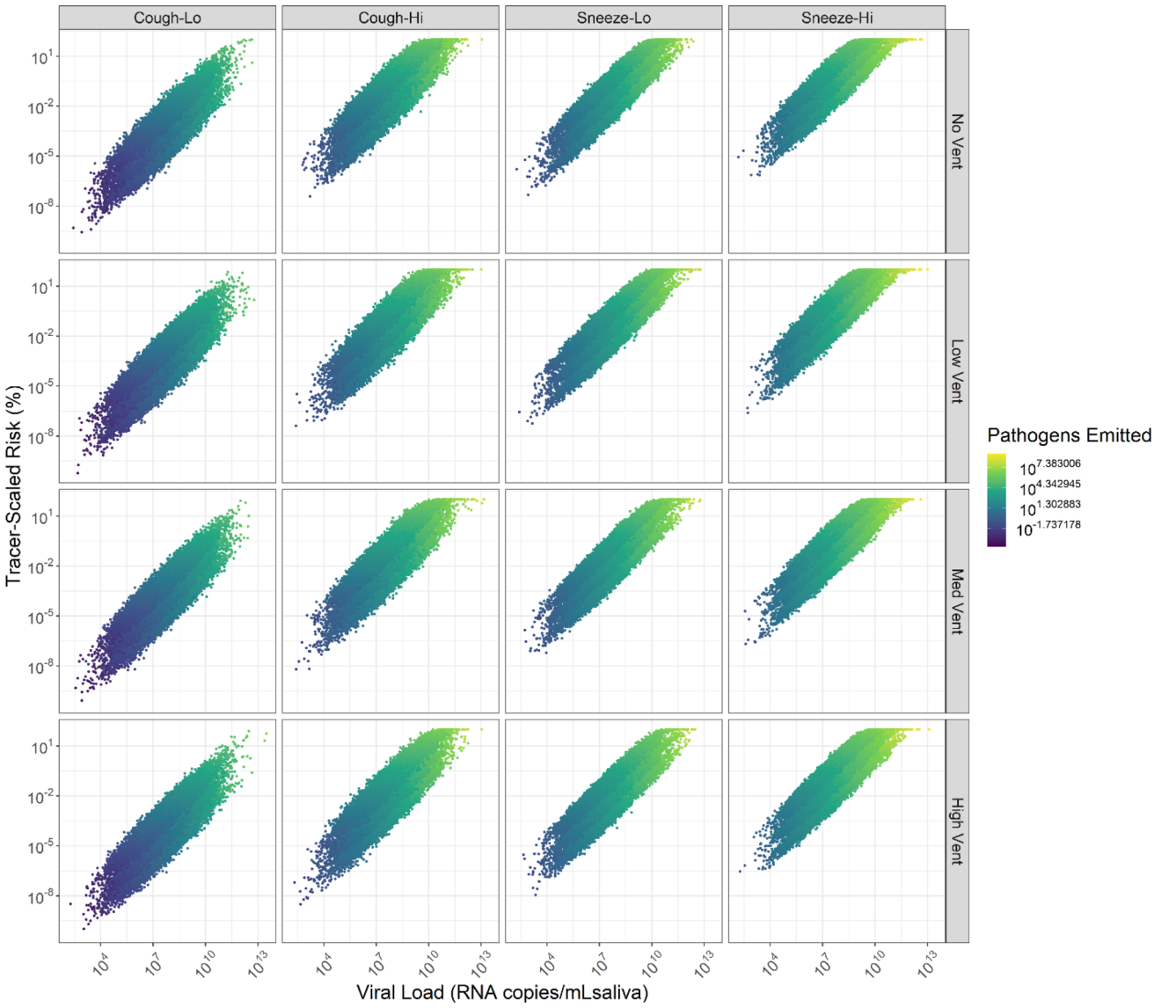

Figure 2. Input−output relationship between tracer-scaled risk and viral load, grouped by mode of emission (columns) and ventilation intervention (rows).

medium or high ventilation as an intervention on risk was modeled.

2.6. Case Study Modeling and Data Analysis. Case study data from an ambulatory care room where DNA tracer measurements were collected before and after installation of a HEPA air cleaner were used to evaluate whether the model could simulate the changes in tracer concentrations resulting from the intervention and whether it is necessary to collect post-intervention tracer measurements to confirm the effectiveness of the air cleaner. DNA tracer decay testing was conducted in an ambulatory care room containing a HEPA air cleaner with a clean air delivery rate (CADR) of 6.3 m^3/min (NSF-X1, Aurabeat AG+). A single emission point and sampling point were placed on different sides of the room ~6 m apart. Filter samples were collected from 45 to 50 min, from 50 to 55 min, and from 55 to 60 min, and DNA tracer decay rates were derived from the slope of a line fit between an initial room concentration, estimated on the basis of tracer aerosolized volume and concentration in a perfectly mixed room (same as the initial concentration of n_{trc} mentioned above), and the final concentration from the 55−60 min sample, using natural log-transformed tracer concentrations. Decay testing was conducted with the air cleaner turned off and turned on with two DNA tracer batches with different tracer concentrations in the solution.

Tracer concentration time series were assumed on the basis of the tracer decay rate, and $c_{trc,meas}$ was estimated by integrating the tracer concentration time series and dividing by the sampling time. Four scenarios were assessed: (1) HEPA Off, Measured, using the measured decay rate from when the HEPA air cleaner was turned off; (2) HEPA On, Measured, using the measured decay rate from when the HEPA air cleaner was turned on; (3) HEPA On, Model Actual, using the HEPA Off, Measured case and modeling the addition of an air cleaning intervention (λ_{int}) equal to the difference in tracer decay rates from the HEPA Off, Measured and HEPA On, Measured cases; and (4) HEPA On, Model Claim, using the HEPA Off, Measured case and modeling the addition of an air cleaning intervention equivalent to the claimed CADR of the HEPA air cleaner. Table S7 summarizes the case study

https://doi.org/10.1021/acs.est.2c08131
Environ. Sci. Technol. XXXX, XXX, XXX−XXX

parameters that differ from those of the scenario testing described above.

3. RESULTS AND DISCUSSION

3.1. Scenario Testing and Input−Output Correlations: Ventilation. Four levels of ventilation were assessed, with pathogen removal rates ranging from zero ventilation [median $\lambda_{pth} + \lambda_{int} = 0.039$ min^{-1} (2.3 h^{-1})] to baseline low ventilation [$\lambda_{trc} = 0.046$ min^{-1} (2.8 h^{-1}), $\lambda_{int} = 0$ min^{-1}, and $\lambda_{pth} = 0.055$ min^{-1} (3.3 h^{-1})] to adding moderate ventilation [median $\lambda_{pth} + \lambda_{int} = 0.11$ min^{-1} (6.6 h^{-1})] to adding high ventilation [median $\lambda_{pth} + \lambda_{int} = 0.22$ min^{-1} (13.2 h^{-1})]. In the zero ventilation case, the pathogen removal rate is the sum of the biological removal rate [$\lambda_{bio} = 0.008$ min^{-1} (0.5 h^{-1})], deposition removal [$\lambda_{trc,chm}(\lambda_{gas} = 0) = 0.031$ min^{-1} (1.9 h^{-1})], and inhalation removal [$\lambda_{pth} = 0.0004$ min^{-1} (0.024 h^{-1})].

Figure 1 summarizes the relationship between tracer concentrations and infection risk for the four modes of emission and four simulated ventilation rates. The red horizontal line indicates 0.1% risk, a target risk value suggested by Buonanno et al. on the basis of the SARS-CoV-2 mortality rate being ∼1 order of magnitude lower than values used in carcinogenic disease mortality, where target reference risk defined by the U.S. Environmental Protection Agency ranges from 0.01% to 0.0001%.[9] Median and 90th percentile tracer-scaled dose and associated risk are plotted on the dose−response curve in Figure S2. We interpret 90th percentiles as indicating risk from a superspreading event, resulting from simulating individuals with elevated viral load and respiratory aerosol emission volume, based on an estimate of 10% of infectious individuals being responsible for ∼80% of SARS-CoV-2 transmission events, though there is no widely accepted definition for SARS-CoV-2 superspreading.[47]

The median respiratory aerosol volumes emitted from the Cough-Hi and Sneeze-Lo emissions are on the same order of magnitude, as is the associated risk, while the volumes emitted from the Cough-Lo and Sneeze-Hi emissions were ∼1.5 orders of magnitude lower and higher, respectively, than the Cough-Hi and Sneeze-Lo events. Only at the highest tracer concentration, when the tracer scaling factor is near unity (0.97), with no or low ventilation does the Cough-Lo scenario pose a risk above 0.1% in the 10th to 90th percentile range. At the highest simulated tracer concentrations, the median tracer-scaled risk for a large-volume cough event with no added ventilation was 0.31%, with 75th and 90th percentiles of 2.4% and 14%, respectively. With high ventilation, the median and 90th percentile risks decrease to 0.07% and 4%, respectively, for a large-volume coughing event and the highest tracer concentration, suggesting additional interventions would be required to reduce near-field superspreader risk below 0.1%.

Just below the upper asymptote of the dose−response curve and above the low-dose region, risk scales linearly with measured tracer concentrations, and as a result, 1 and 2 log 10 reductions in tracer concentrations resulted in similar reductions in risk. For example, the median tracer-scaled risk for a large-volume cough event with no added ventilation decreased from 0.31% at 3.7×10^5 DNA copies/L of air to 0.03% with a tracer concentration of 3.7×10^4 DNA copies/L of air.

The relative impact of ventilation is compared by calculating relative risk using the low-ventilation condition with no added ventilation as a baseline. Relative risk values were relatively consistent as measured tracer concentrations and mode of emission varied. As shown in Figure S3, when ventilation is reduced to zero, the median relative risk is increased by 30 ± 8%, averaged (±standard deviation) across tracer concentrations and emission modes. Increasing ventilation by adding 3.5 and 10 h^{-1} of aerosol removal reduced the relative risk by 50 ± 4% and 74 ± 1%, respectively. Increasing ventilation increases the removal rate of an initial spike of pathogens resulting from an impulse emission, and therefore, the relative risk reduction resulting from ventilation interventions on impulse emissions tends to be different than for continuous emissions, where ventilation decreases steady state pathogen concentrations.

The variability in risk estimates is mainly driven by the variability in viral load and respiratory aerosol volume emitted, as distributions for these parameters vary over multiple orders of magnitude. Figure 2 demonstrates the relationship between viral load and risk for each simulation. Stratification of risk in Figure 2 indicates the three simulated tracer concentrations. Spearman rank correlations between viral load and risk range from 0.96 to 0.98, while correlations between respiratory aerosol volume and risk range from 0.15 to 0.28. Correlations between θ_{inf} and risk range from 0.07 to 0.11. Figure S4 visualizes the relationship among viral load, respiratory aerosol volume, and total pathogens emitted. As shown in Figure S5, for each ventilation scenario, emission mode, and measured tracer concentration, there is a threshold of the number of pathogens emitted resulting in a significant increase in the range of predicted risk.

Section S7 summarizes the impact of occupancy and masking on risk, and Section S8 describes dose−response curve testing.

3.2. Scenario Testing: Layering Interventions. Layering interventions is an effective method of reducing SARS-CoV-2 transmission risk, especially in high-occupancy settings.[48,49] We quantify the impact of layering interventions by simulating six scenarios ranging from a high-risk scenario with a high occupant density to low ventilation and no masking to a lower-risk scenario with medium occupant density, adding medium-high ventilation (5 h^{-1}), and surgical masking. Figure S11 shows the reduction in absolute risk as interventions are applied, and relative risk reduction compared to the high-risk scenario is plotted in Figure S12. In the Cough-Hi scenario, adding medium-high ventilation and reducing occupancy reduced the median risk to 0.1% at the highest tracer concentration. When surgical masks are layered in addition to lower occupancy and increased ventilation, the risk of transmission from a superspreader remains above the 0.1% threshold, suggesting more aggressive interventions would be required to reach this risk target. Compared to the high-risk scenario, reducing the occupancy from 30 to 10 reduced the relative risk by 66 ± 2% and adding 5 h^{-1} of intervention ventilation reduced the relative risk by 58 ± 2%. Layering reduced occupancy with increased ventilation reduced relative risk by 86 ± 1%, and adding surgical masks resulted in a 98 ± 0.1% reduction in relative risk.

3.3. Scenario Testing: Guangzhou Restaurant Outbreak. Figure S13 summarizes the analysis of a SARS-CoV-2 outbreak in a restaurant in Guangzhou, China. The pathogen removal rate was estimated to be 0.057 min^{-1} (3.4 h^{-1}) in this scenario, compared to a tracer removal rate of 0.048 min^{-1} (2.9 h^{-1}), calculated using the outdoor air supply flow rate and room volume with eq S1. At the highest simulated tracer concentrations, corresponding to a tracer scaling factor of 3.3,

https://doi.org/10.1021/acs.est.2c08131
Environ. Sci. Technol. XXXX, XXX, XXX−XXX

the median tracer-scaled risk for a large-volume cough event with no added ventilation (λ_{int} = 0 min^{-1}) in the restaurant was 2.1%, with 75th and 90th percentiles of 15% and 63%, respectively. Parhizkar et al. estimated an inhalation dose of 11 PFUs based on an attack rate of 47.6%,[45] a value within the 75th to 90th percentile range of the tracer-scaled model. Adding 3.5 and 10 h^{-1} of ventilation in this scenario was estimated to reduce the median relative risk by 51 ± 2% and 74 ± 1%, respectively, though significant superspreader risk remained.

3.4. Case Study: Ambulatory Care Room. The tracer-scaled QMRA model was used to estimate the risk of infection inside an ambulatory care room using measured tracer concentrations. Without the HEPA air cleaner operating, the pathogen removal rate was estimated to be 0.09 min^{-1} (5.4 h^{-1}), with a measured tracer removal rate of 0.08 min^{-1} (4.7 h^{-1}). Turning on the HEPA air cleaner increased the pathogen removal rate to 0.13 min^{-1} (7.8 h^{-1}), though on the basis of the CADR of the HEPA air cleaner, the removal rate would be expected to be 0.14 min^{-1} (8.4 h^{-1}). Table S8 summarizes the absolute risk values, as well as relative risk reductions compared to those of the HEPA Off, Measured scenario. The median absolute risk is <0.1% for all modes of emission, except Sneeze-Hi, regardless of intervention performance, partially due to the space having a ventilation rate comparable to the medium-high ventilation rate from scenario testing prior to turning on the HEPA air cleaner. Average relative risk reduction from measurements of turning on the HEPA air cleaner was 30 ± 3%. The average difference in median relative risk reduction predicted from the measured and modeled operation of the HEPA air cleaner was 1.7%, demonstrating comparability between modeling and measuring the impact of this intervention, despite using tracer batches with different tracer concentrations in solution when testing the HEPA Off, Measured and HEPA On, Measured scenarios. Modeling the claimed CADR of the HEPA air cleaner resulted in overestimating median relative risk reductions by 6−8%.

The impact of the intervention on superspreader risk was somewhat inconsistent. While the 90th percentiles of risk from the baseline scenario were consistently higher than for the intervention scenarios, the scenario with the highest ventilation rate (HEPA On, Model Claimed) was not always the scenario with the lowest 90th percentile of absolute or relative risk (e.g., Cough-Hi). As shown in input−output correlation analysis described above, this observed inconsistency is impacted by the variability in sampling the extremes of the viral load and respiratory aerosol volume distributions, despite running 10 000 simulations for each scenario, as well as the relative similarities in intervention removal rates between tested scenarios.

3.5. Limitations of the Tracer-Scaled Bulk Aerosol QMRA Model. The tracer-scaled bulk aerosol QMRA model has multiple limitations that may be improved with more complex modeling schemes and improved constraints on input parametrizations. Treating aerosols as a bulk substance does not account for differential removal of larger aerosol particles due to deposition, and particles of increasing size could be more enriched with tracers and/or pathogens following the evaporation process, leading to potential discrepancies in bulk aerosol removal estimates. An additional factor correcting for discrepancies between tracer and pathogen bulk removal rates resulting from differences in size distributions may be derived with further testing. A particle size-resolved model could improve the accuracy of aerosol transport modeling, accounting for the particle size dependence of emission, removal rates, and inhalation deposition.[8,50] Incorporating tracer measurements into such a model requires particle size selective filter sampling equipment.

We considered only impulse modes of respiratory emission, matching how the tracer is currently deployed. This framework can be adopted to continuous respiratory emissions if a continuous tracer emission scheme is developed. Impulse events are likely drivers of superspreading events due to the large respiratory aerosol volumes emitted, making this tool useful in assessing risk mitigation strategies in such situations.

Assumptions were made regarding respiratory aerosol transport being consistent with tracer transport, and more accurately recreating the particle size distribution, emission velocity, and aerosol volume of tracer emissions may improve the accuracy of this assumption. Respiratory aerosol emission volume distributions are based on historical measurements, but measurements using modern tools that accurately measure the entire size distribution of respiratory aerosols and their physicochemical changes during transport are needed for impulse emissions. The impulse emission aerosol volume variability over repeated emission events can be better parametrized with experimental data when available. We do not compare differences in air velocity between respiratory and tracer aerosol emissions, though this factor can be important in determining the spatial transport of aerosols indoors, especially in poorly mixed spaces. While not practical for use in commercial applications of the tracer, a cough simulator could improve tracer emission comparability with a physiologically realistic cough.[51] When ventilation interventions are modeled, changes in mixing effectiveness that may result are not currently simulated.

The dose−response determination was performed in individuals without prior vaccination or infection. Individuals with partial immunity may require a larger dose for infection, for which this model does not account. In addition, the static QMRA model described here does not account for population-scale aspects of transmission risk (e.g., secondary spread), though this model could be expanded into a dynamic QMRA.[52−54]

DNA tracers are promising candidates for environmental modeling as it is not feasible to measure multiple pathogen targets due to challenges associated with low biomass, recovery, and pathogen exposure during testing. DNA tracers are nonpathogenic and nontoxic, allowing testing in occupied spaces. A limitation of DNA tracers is that they do not simulate pathogen inactivation during emission and transport, as the DNA tracer is stable in aerosolized form, and this factor must be accounted for using parametrizations for the fraction of pathogens that survive aerosolization and the biological decay rate. Measurements of SARS-CoV-2 and DNA tracer decay concurrently would be useful in confirming the parametrization of pathogen biological and physical removal compared to tracer physical removal. A benefit of the environmental stability of this DNA tracer is that with accurate pathogen physical and biological removal parametrizations, one tracer test can predict risk from multiple different pathogens by adjusting model inputs accordingly.

https://doi.org/10.1021/acs.est.2c08131
Environ. Sci. Technol. XXXX, XXX, XXX−XXX

■ ASSOCIATED CONTENT

Supporting Information

The Supporting Information is available free of charge at https://pubs.acs.org/doi/10.1021/acs.est.2c08131.

Distributions of the respiratory aerosol emission volume (Section S1), distributions of viral load in respiratory aerosols (Section S2), inhalation rate distribution (Section S3), tracer emission analysis, (Section S4), DNA tracer filter sampling and quantification (Section S5), estimating tracer removal rates with gaseous tracers or ventilation rate (Section S6), scenario testing, occupancy, and masking (Section S7), scenario testing and dose−response curve (Section S8), normalized particle number distribution of the tracer nebulizer compared to the BLO model (Figure S1), tracer-scaled risk versus tracer-scaled dose for each mode of emission (Figure S2), relative risk under various ventilation conditions (Figure S3), relationship among the number of pathogens emitted, viral load, and respiratory aerosol volume (Figure S4), relationship among tracer-scaled risk, the number of pathogens emitted, and measured tracer concentrations (Figure S5), tracer-scaled risk versus measured tracer concentrations as occupancy is varied (Figure S6), relative risk as occupancy is varied (Figure S7), tracer-scaled risk versus measured tracer concentrations as masking is varied (Figure S8), relative risk as masking is varied (Figure S9), tracer-scaled risk versus measured tracer concentrations as dose−response parameters are varied (Figure S10), tracer-scaled risk versus measured tracer concentrations as layered interventions are varied (Figure S11), relative risk as layered interventions are varied (Figure S12), tracer-scaled risk versus measured tracer concentrations as ventilation is varied for the Guangzhou restaurant scenario (Figure S13), respiratory emission volume distribution percentiles (Table S1), respiratory aerosol volume emission parametrizations (Table S2), tidal inhalation rate distribution percentiles (Table S3), respiratory pathogen:DNA tracer emission ratios (Table S4), Monte Carlo simulation parameters for the tracer-scaled QMRA model (Table S5), scenario testing model inputs (Table S6), Monte Carlo simulation parameters for the case study evaluation of the tracer-scaled QMRA model (Table S7), and case study results of risk estimation (Table S8) (PDF)

■ AUTHOR INFORMATION

Corresponding Author

Nicholas Clements − *Paul M. Rady Department of Mechanical Engineering, University of Colorado at Boulder, Boulder, Colorado 80309, United States;* orcid.org/0000-0003-3577-579X; Email: nicholas.clements@colorado.edu

Authors

Ilan Arvelo − *SafeTraces, Inc., Pleasanton, California 94588, United States*

Phil Arnold − *SafeTraces, Inc., Pleasanton, California 94588, United States*

Nicholas J. Heredia − *SafeTraces, Inc., Pleasanton, California 94588, United States*

Ulrike W. Hodges − *SafeTraces, Inc., Pleasanton, California 94588, United States*

Stan Deresinski − *Stanford University School of Medicine, Stanford, California 94305, United States*

Peter W. Cook − *Independent researcher, Atlanta, Georgia 30333, United States*

Kerry A. Hamilton − *School of Sustainable Engineering and the Built Environment and The Biodesign Institute Center for Environmental Health Engineering, Arizona State University, Tempe, Arizona 85281, United States;* orcid.org/0000-0003-2991-7325

Complete contact information is available at: https://pubs.acs.org/10.1021/acs.est.2c08131

Notes

The authors declare no competing financial interest.

■ ACKNOWLEDGMENTS

The authors acknowledge and appreciate feedback and discussions from colleagues at SafeTraces (Erik Malmstrom) and RHP Risk Management Inc. (Frank Pagone and Jacob Persky). This work was funded by Air Force (AF) Small Business Technology Transfer (STTR) AF21B-TCSO1 Phase I Proposal FX21B-TCSO1-0317.

■ REFERENCES

(1) Wang, C. C.; Prather, K. A.; Sznitman, J.; Jimenez, J. L.; Lakdawala, S. S.; Tufekci, Z.; Marr, L. C. Airborne Transmission of Respiratory Viruses. *Science* **2021**, *373* (6558), No. eabd9149.

(2) Tellier, R. COVID-19: The Case for Aerosol Transmission. *Interface Focus.* **2022**, *12* (2), 20210072.

(3) Tellier, R. Review of Aerosol Transmission of Influenza A Virus. *Emerg. Infect. Dis.* **2006**, *12* (11), 1657−1662.

(4) ASHRAE Epidemic Task Force. Core Recommendations for Reducing Airborne Infectious Aerosol Exposure. 2021.

(5) AIHA. Reducing the Risk of COVID-19 Using Engineering Controls. 2020.

(6) Infection Prevention and Control (IPC) in Health-Care Facilities in the Event of a Surge or Resurgence in Cases of COVID-19. World Health Organization: Geneva, 2021; p 4. https://apps.who.int/iris/handle/10665/350647 (accessed 2022-04-06).

(7) Schijven, J.; Vermeulen, L. C.; Swart, A.; Meijer, A.; Duizer, E.; de Roda Husman, A. M. Quantitative Microbial Risk Assessment for Airborne Transmission of SARS-CoV-2 via Breathing, Speaking, Singing, Coughing, and Sneezing. *Environ. Health Perspect* **2021**, *129* (4), 047002.

(8) Henriques, A.; Mounet, N.; Aleixo, L.; Elson, P.; Devine, J.; Azzopardi, G.; Andreini, M.; Rognlien, M.; Tarocco, N.; Tang, J. Modelling Airborne Transmission of SARS-CoV-2 Using CARA: Risk Assessment for Enclosed Spaces. *Interface Focus* **2022**, DOI: 10.1098/rsfs.2021.0076.

(9) Buonanno, G.; Morawska, L.; Stabile, L. Quantitative Assessment of the Risk of Airborne Transmission of SARS-CoV-2 Infection: Prospective and Retrospective Applications. *Environ. Int.* **2020**, *145*, 106112.

(10) Harding, R. N.; Hara, C. A.; Hall, S. B.; Vitalis, E. A.; Thomas, C. B.; Jones, A. D.; Day, J. A.; Tur-Rojas, V. R.; Jorgensen, T.; Herchert, E.; Yoder, R.; Wheeler, E. K.; Farquar, G. R. Unique DNA-Barcoded Aerosol Test Particles for Studying Aerosol Transport. *Aerosol Sci. Technol.* **2016**, *50* (5), 429−435.

(11) Arvelo, I.; Pagone, F.; Persky, J.; Carpio, C. E.; Arnold, P.; Clements, N. Decay Rates of Two Tracer Gases Compared to DNA-Tagged Liquid Aerosol Tracer Particles: Impact of Varying Dilution Rate and Filtration. *Building and Environment* **2022**, *212*, 108819.

(12) Mousavi, E.; Grosskopf, K.; Arnold, P.; Lautz, R.; Lau, J. Experimental Measurement of Bioaerosol Concentrations and Containment in Long-Term Care Environments. *Building and Environment* **2022**, *223*, 109415.

https://doi.org/10.1021/acs.est.2c08131
Environ. Sci. Technol. XXXX, XXX, XXX−XXX

(13) Haas, C. N.; Rose, J. B.; Gerba, C. P. *Quantitative Microbial Risk Assessment*, 2nd ed.; John Wiley & Sons, Inc.: New York, 2014.
(14) Bagheri, G.; Thiede, B.; Hejazi, B.; Schlenczek, O.; Bodenschatz, E. An Upper Bound on One-to-One Exposure to Infectious Human Respiratory Particles. *Proc. Natl. Acad. Sci. U.S.A.* **2021**, *118* (49), No. e2110117118.
(15) Ai, Z.; Hashimoto, K.; Melikov, A. K. Airborne Transmission between Room Occupants during Short-term Events: Measurement and Evaluation. *Indoor Air* **2019**, ina.12557.
(16) Good, N.; Fedak, K. M.; Goble, D.; Keisling, A.; L'Orange, C.; Morton, E.; Phillips, R.; Tanner, K.; Volckens, J. Respiratory Aerosol Emissions from Vocalization: Age and Sex Differences Are Explained by Volume and Exhaled CO $_2$. *Environ. Sci. Technol. Lett.* **2021**, *8* (12), 1071−1076.
(17) Kappelt, N.; Russell, H. S.; Kwiatkowski, S.; Afshari, A.; Johnson, M. S. Correlation of Respiratory Aerosols and Metabolic Carbon Dioxide. *Sustainability* **2021**, *13* (21), 12203.
(18) Bueno de Mesquita, P. J.; Noakes, C. J.; Milton, D. K. Quantitative Aerobiologic Analysis of an Influenza Human Challenge-transmission Trial. *Indoor Air* **2020**, *30* (6), 1189−1198.
(19) Lu, Y.; Li, Y.; Zhou, H.; Lin, J.; Zheng, Z.; Xu, H.; Lin, B.; Lin, M.; Liu, L. Affordable Measures to Monitor and Alarm Nosocomial SARS-CoV-2 Infection Due to Poor Ventilation. *Indoor Air* **2021**, *31* (6), 1833−1842.
(20) Kumar, P.; Omidvarborna, H.; Tiwari, A.; Morawska, L. The Nexus between In-Car Aerosol Concentrations, Ventilation and the Risk of Respiratory Infection. *Environ. Int.* **2021**, *157*, 106814.
(21) Eilts, S. M.; Li, L.; Pope, Z. C.; Hogan, C. J. Characterization of Exhaled Particle Deposition and Ventilation in an Indoor Setting. *Atmos. Environ.* **2021**, *262*, 118602.
(22) Aganovic, A.; Bi, Y.; Cao, G.; Drangsholt, F.; Kurnitski, J.; Wargocki, P. Estimating the Impact of Indoor Relative Humidity on SARS-CoV-2 Airborne Transmission Risk Using a New Modification of the Wells-Riley Model. *Building and Environment* **2021**, *205*, 108278.
(23) Aydin, M.; Savas, S. A.; Evrendilek, F.; Aydin, I. E.; Evrendilek, D. E. A Model for Indoor Motion Dynamics of SARS-CoV-2 as a Function of Respiratory Droplet Size and Evaporation. *Environ. Monit Assess* **2021**, *193* (10), 626.
(24) Liu, L.; Wei, J.; Li, Y.; Ooi, A. Evaporation and Dispersion of Respiratory Droplets from Coughing. *Indoor Air* **2017**, *27* (1), 179−190.
(25) Bourouiba, L. Fluid Dynamics of Respiratory Infectious Diseases. *Annu. Rev. Biomed. Eng.* **2021**, *23* (1), 547−577.
(26) Vejerano, E. P.; Marr, L. C. Physico-Chemical Characteristics of Evaporating Respiratory Fluid Droplets. *J. R. Soc. Interface.* **2018**, *15* (139), 20170939.
(27) Killingley, B.; Mann, A. J.; Kalinova, M.; Boyers, A.; Goonawardane, N.; Zhou, J.; Lindsell, K.; Hare, S. S.; Brown, J.; Frise, R.; Smith, E.; Hopkins, C.; Noulin, N.; Löndt, B.; Wilkinson, T.; Harden, S.; McShane, H.; Baillet, M.; Gilbert, A.; Jacobs, M.; Charman, C.; Mande, P.; Nguyen-Van-Tam, J. S.; Semple, M. G.; Read, R. C.; Ferguson, N. M.; Openshaw, P. J.; Rapeport, G.; Barclay, W. S.; Catchpole, A. P.; Chiu, C. Safety, Tolerability and Viral Kinetics during SARS-CoV-2 Human Challenge in Young Adults. *Nat. Med.* **2022**, *28*, 1031.
(28) Exposure Factors Handbook 2011 ed. (Final Report). EPA/600/R-09/052F; U.S. Environmental Protection Agency: Washington, DC, 2011; p 1436.
(29) Dabisch, P.; Schuit, M.; Herzog, A.; Beck, K.; Wood, S.; Krause, M.; Miller, D.; Weaver, W.; Freeburger, D.; Hooper, I.; Green, B.; Williams, G.; Holland, B.; Bohannon, J.; Wahl, V.; Yolitz, J.; Hevey, M.; Ratnesar-Shumate, S. The Influence of Temperature, Humidity, and Simulated Sunlight on the Infectivity of SARS-CoV-2 in Aerosols. *Aerosol Sci. Technol.* **2021**, *55* (2), 142−153.
(30) Miller, S. L.; Nazaroff, W. W.; Jimenez, J. L.; Boerstra, A.; Buonanno, G.; Dancer, S. J.; Kurnitski, J.; Marr, L. C.; Morawska, L.; Noakes, C. Transmission of SARS-CoV-2 by Inhalation of Respiratory Aerosol in the Skagit Valley Chorale Superspreading Event. *Indoor Air* **2021**, *31* (2), 314−323.
(31) Chan, K.-H.; Sridhar, S.; Zhang, R. R.; Chu, H.; Fung, A. Y.-F.; Chan, G.; Chan, J. F.-W.; To, K. K.-W.; Hung, I. F.-N.; Cheng, V. C.-C.; Yuen, K.-Y. Factors Affecting Stability and Infectivity of SARS-CoV-2. *Journal of Hospital Infection* **2020**, *106* (2), 226−231.
(32) Kreutzberger, A. J. B.; Sanyal, A.; Saminathan, A.; Bloyet, L.-M.; Stumpf, S.; Liu, Z.; Ojha, R.; Patjas, M. T.; Geneid, A.; Scanavachi, G.; Doyle, C. A.; Somerville, E.; Correia, R. B. D. C.; Di Caprio, G.; Toppila-Salmi, S.; Mäkitie, A.; Kiessling, V.; Vapalahti, O.; Whelan, S. P. J.; Balistreri, G.; Kirchhausen, T. SARS-CoV-2 Requires Acidic PH to Infect Cells. *Proc. Natl. Acad. Sci. U.S.A.* **2022**, *119* (38), No. e2209514119.
(33) Johnson, G. R.; Morawska, L.; Ristovski, Z. D.; Hargreaves, M.; Mengersen, K.; Chao, C. Y. H.; Wan, M. P.; Li, Y.; Xie, X.; Katoshevski, D.; Corbett, S. Modality of Human Expired Aerosol Size Distributions. *J. Aerosol Sci.* **2011**, *42* (12), 839−851.
(34) Zhao, L.; Qi, Y.; Luzzatto-Fegiz, P.; Cui, Y.; Zhu, Y. COVID-19: Effects of Environmental Conditions on the Propagation of Respiratory Droplets. *Nano Lett.* **2020**, *20* (10), 7744−7750.
(35) Shen, Y.; Courtney, J. M.; Anfinrud, P.; Bax, A. Hybrid Measurement of Respiratory Aerosol Reveals a Dominant Coarse Fraction Resulting from Speech That Remains Airborne for Minutes. *Proc. Natl. Acad. Sci. U.S.A.* **2022**, *119* (26), No. e2203086119.
(36) Morawska, L.; Johnson, G. R.; Ristovski, Z. D.; Hargreaves, M.; Mengersen, K.; Corbett, S.; Chao, C. Y. H.; Li, Y.; Katoshevski, D. Size Distribution and Sites of Origin of Droplets Expelled from the Human Respiratory Tract during Expiratory Activities. *J. Aerosol Sci.* **2009**, *40* (3), 256−269.
(37) R Core Team. *R: A Language and Environment for Statistical Computing*; 2022. https://www.R-project.org/.
(38) Lindsley, W. G.; Pearce, T. A.; Hudnall, J. B.; Davis, K. A.; Davis, S. M.; Fisher, M. A.; Khakoo, R.; Palmer, J. E.; Clark, K. E.; Celik, I.; Coffey, C. C.; Blachere, F. M.; Beezhold, D. H. Quantity and Size Distribution of Cough-Generated Aerosol Particles Produced by Influenza Patients During and After Illness. *Journal of Occupational and Environmental Hygiene* **2012**, *9* (7), 443−449.
(39) Duguid, J. P. The Size and the Duration of Air-Carriage of Respiratory Droplets and Droplet-Nuclei. *Epidemiol. Infect.* **1946**, *44* (6), 471−479.
(40) Gerone, P. J.; Couch, R. B.; Keefer, G. V.; Douglas, R. G.; Derrenbacher, E. B.; Knight, V. Assessment of Experimental and Natural Viral Aerosols. *Bacteriol. Rev.* **1966**, *30* (3), 576−588.
(41) Jacot, D.; Greub, G.; Jaton, K.; Opota, O. Viral Load of SARS-CoV-2 across Patients and Compared to Other Respiratory Viruses. *Microbes and Infection* **2020**, *22* (10), 617−621.
(42) Lednicky, J. A.; Lauzardo, M.; Fan, Z. H.; Jutla, A.; Tilly, T. B.; Gangwar, M.; Usmani, M.; Shankar, S. N.; Mohamed, K.; Eiguren-Fernandez, A.; Stephenson, C. J.; Alam, Md. M.; Elbadry, M. A.; Loeb, J. C.; Subramaniam, K.; Waltzek, T. B.; Cherabuddi, K.; Morris, J. G.; Wu, C.-Y. Viable SARS-CoV-2 in the Air of a Hospital Room with COVID-19 Patients. *International Journal of Infectious Diseases* **2020**, *100*, 476−482.
(43) Koh, X. Q.; Sng, A.; Chee, J. Y.; Sadovoy, A.; Luo, P.; Daniel, D. Outward and Inward Protection Efficiencies of Different Mask Designs for Different Respiratory Activities. *J. Aerosol Sci.* **2022**, *160*, 105905.
(44) Marr, L. C.; Tang, J. W.; Van Mullekom, J.; Lakdawala, S. S. Mechanistic Insights into the Effect of Humidity on Airborne Influenza Virus Survival, Transmission and Incidence. *J. R. Soc. Interface.* **2019**, *16* (150), 20180298.
(45) Parhizkar, H.; Van Den Wymelenberg, K. G.; Haas, C. N.; Corsi, R. L. A Quantitative Risk Estimation Platform for Indoor Aerosol Transmission of COVID-19. *Risk Analysis* **2022**, *42*, 2075−2088.
(46) Li, Y.; Qian, H.; Hang, J.; Chen, X.; Cheng, P.; Ling, H.; Wang, S.; Liang, P.; Li, J.; Xiao, S.; Wei, J.; Liu, L.; Cowling, B. J.; Kang, M. Probable Airborne Transmission of SARS-CoV-2 in a Poorly Ventilated Restaurant. *Building and Environment* **2021**, *196*, 107788.

https://doi.org/10.1021/acs.est.2c08131
Environ. Sci. Technol. XXXX, XXX, XXX−XXX

(47) Cave, E. COVID-19 Super-Spreaders: Definitional Quandaries and Implications. *ABR* **2020**, *12* (2), 235−242.
(48) Brooks-Pollock, E.; Christensen, H.; Trickey, A.; Hemani, G.; Nixon, E.; Thomas, A. C.; Turner, K.; Finn, A.; Hickman, M.; Relton, C.; Danon, L. High COVID-19 Transmission Potential Associated with Re-Opening Universities Can Be Mitigated with Layered Interventions. *Nat. Commun.* **2021**, *12* (1), 5017.
(49) Leech, G.; Rogers-Smith, C.; Monrad, J. T.; Sandbrink, J. B.; Snodin, B.; Zinkov, R.; Rader, B.; Brownstein, J. S.; Gal, Y.; Bhatt, S.; Sharma, M.; Mindermann, S.; Brauner, J. M.; Aitchison, L. Mask Wearing in Community Settings Reduces SARS-CoV-2 Transmission. *Proc. Natl. Acad. Sci. U.S.A.* **2022**, *119* (23), No. e2119266119.
(50) Lai, J.; Coleman, K. K.; Tai, S.-H. S.; German, J.; Hong, F.; Albert, B.; Esparza, Y.; Srikakulapu, A. K.; Schanz, M.; Maldonado, I. S.; Oertel, M.; Fadul, N.; Gold, T. L.; Weston, S.; Mullins, K.; McPhaul, K. M.; Frieman, M.; Milton, D. K. Exhaled Breath Aerosol Shedding by Highly Transmissible Versus Prior SARS-CoV-2 Variants. *Clin. Infect. Dis.* **2023**, *76*, 786−794.
(51) Lindsley, W. G.; Reynolds, J. S.; Szalajda, J. V.; Noti, J. D.; Beezhold, D. H. A Cough Aerosol Simulator for the Study of Disease Transmission by Human Cough-Generated Aerosols. *Aerosol Sci. Technol.* **2013**, *47* (8), 937−944.
(52) Olivieri, A. W.; Seto, E. Y.; Danielson, R. E.; Soller, J. A.; Cooper, R. C. Applications of Quantitative Microbial Risk Assessment (QMRA) to Regulatory Decision Making.
(53) Amoueyan, E.; Ahmad, S.; Eisenberg, J. N. S.; Gerrity, D. A Dynamic Quantitative Microbial Risk Assessment for Norovirus in Potable Reuse Systems. *Microbial Risk Analysis* **2020**, *14*, 100088.
(54) Brouwer, A. F.; Masters, N. B.; Eisenberg, J. N. S. Quantitative Microbial Risk Assessment and Infectious Disease Transmission Modeling of Waterborne Enteric Pathogens. *Curr. Envir Health Rpt* **2018**, *5* (2), 293−304.

https://doi.org/10.1021/acs.est.2c08131
Environ. Sci. Technol. XXXX, XXX, XXX−XXX